Journal of the Brazilian Chemical Society
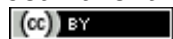
Article

Down- and Up-Conversion Photoluminescence of Carbon-Dots from Brewing Industry Waste: Application in Live Cell-Imaging Experiments

Carime V. Rodrigues,[*,a] *José R. Correa,*[b] *Carlos M. Aiube,*[a] *Lorena P. Andrade,*[b] *Pedro M. Galvão,*[a] *Pâmela A. Costa,*[a] *Ariadna L. Campos,*[a] *Anderson J. Pereira,*[c] *Grace F. Ghesti,*[d] *Jorlandio F. Felix,*[c,e] *Ingrid T. Weber,*[a] *Brenno A. Neto*[b] *and Marcelo O. Rodrigues*[a]

[a]*Laboratório de Inorgânica e Materiais (LIMA), Instituto de Química (IQ),* [b]*Laboratório de Química Medicinal e Tecnológica (LaQuiMeT), IQ,* [c]*Núcleo de Física Aplicada, Instituto de Física (IF) and* [d]*Laboratório de Catálise (LABCAT), IQ, Universidade de Brasília (UnB), Campus Universitário Darcy Ribeiro, 70904-970 Brasilia-DF, Brazil*

[e]*Departamento de Física, Universidade Federal de Viçosa (UFV), 36570-900 Viçosa-MG, Brazil*

Simple synthetic procedures have been applied to obtain luminescent carbon quantum dots, also referred as C-dots, from an abundant carbon source, that is, from the brewing industry waste. The synthetic procedures have been conducted aiming to investigate the effects of the oxidation stage on the properties of the nanomaterial. C-dots down- and up-conversion properties, as well as their potential for cellular imaging experiments in live (and adhered) cells, are disclosed herein.

Keywords: C-dots, luminescence, up-conversion, live cell-imaging

Introduction

The development of new photoluminescent nanomaterials has attracted much attention over the last decades because of their advantageous properties in comparison to those presented by conventional bulk materials. These nanomaterials have a tremendous impact over a wide range of strategic fields, such as diagnostic, therapeutic, electronic, photonic and energy.[1] Among well-established fluorescent nanomaterials, the class of the so-called quantum dots (QDs), based on heavy metal elements, may be considered as one of the most iconic and prominent materials.[2] Heavy metal QDs exhibit attractive properties, such as tunable emission, photostability and intense bright luminescence, which enable them to be widely explored in both medicine and biology. The presence of toxic elements, such as cadmium, lead or mercury in their compositions has been considered, however, as a huge drawback for furthering their applications as a topic of major concerns.

Carbon quantum dots (known as C-dots) are a new class of fluorescent nanoparticles, which have emerged as a promising alternative to overcome major negative aspects associated with heavy QDs. C-dots have received a special attention, not only because of their optical properties, but also for both their small size and non-toxicity. These features also open a wealth of possibilities toward the development of new optical probes for biological applications.[3,4]

C-dots spectroscopic properties are the subject of many controversies and some mechanisms have been speculated to be responsible for the luminescence of these materials. The presence of energy traps on their surface, which may cause a quantum confinement effect; the energy states associated to edge defects; or even exciton transitions are some possibilities hotly debated.[3]

C-dots can be produced from a variety of synthetic procedures and from a large range of cheap and readily available carbon sources, such as glucose, watermelon rinds,[5] hair[6] and even cow manure.[7] Wort bagasse is a byproduct from brewing process and is a component of the solid material produced from wort filtration before the next steps toward beer manufacture.[8] This byproduct is mainly constituted of leftover peels and pulp of malt, grain and also some additives (wheat, rice and corn, for exemple). Crushed malt is 85% of the total product generated by the brewing industry and is, thus, the most abundant byproduct from this process.[9] Brazil is the third largest beer producer in the world, with a production of 12.6 million liters (ML)

*e-mail: carime.v.rodrigues@gmail.com

while China (40 ML) and the United States (35 ML) have a larger production.[8]

Knowing that brewing residues are admittedly an abundant carbon source, this work aims to explore these materials to synthesize C-dots. We also describe the nanomaterial characterization, down- and up-conversion photoluminescent properties of C-dots obtained through two different methodologies, which are expected to afford C-dots with distinct oxidation degrees. The impact of pH and temperature over the optical properties were also analyzed. The new synthesized C-dots also had their potential for bioimaging experiments using breast cancer cell (MCF-7) lineages tested. Herein, the newly synthesized nanomaterials are designated as **1** and **2**, referring to the more oxidized and less oxidized C-dots, respectively.

Experimental

C-dots **1** were obtained similarly to a previously reported methodology,[7] that is, by chemical oxidation followed by extraction. C-dots **2** were synthesized using a similar methodology, but excluding the oxidation treatment (Scheme 1; a detailed procedure can be found in the Supplementary Information file).
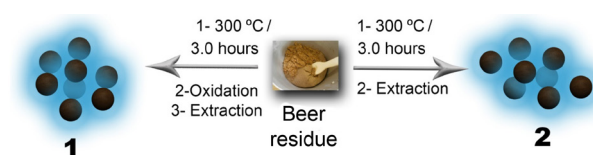
Scheme 1. Synthetic procedures for the synthesis of the studied C-dots **1** and **2**.

The high-resolution transmission electron microscopy (HRTEM) images were obtained in a JEOL JEM 2100 electron microscope (Tokyo, Japan) operating at an accelerating voltage of 200 kV. The aqueous solutions containing the C-dots were deposited on a 400-mesh C-coated copper grid (Ted Pella Inc., Redding, CA, USA) and dried in air. The Fourier transform infrared (FTIR) spectra were recorded from potassium bromide (KBr) pellets, in a spectral range of 4000-400 cm^{-1}, using a Jasco FT/IR-4100 spectrometer (Tokyo, Japan). The zeta potentials were measured using a Zetasizer Nano-ZS90 (Malvern, United Kingdom). The Raman measurements were performed using the Renishaw InVia micro-Raman system (Sheffield, UK) equipped with the 514.5 nm argon laser line and a 50× objective, resulting in a laser spot size of around 1 μm in the focal plane. The laser excitation power was about 0.05 mW at the sample surfaces. The Raman measurements were recorded using C-dots in their powdered form. The fluorescence spectra of the nanomaterials were

acquired using a Lumina fluorescence spectrometer (Thermo Ficher Scientific Inc., Waltham, MA, USA) with a Peltier system to vary the temperature, when necessary. A detailed procedure for the cell-imaging experiments is described in the Supplementary Information file.

Results and Discussion

Brewing residue is an abundant carbon source, considering it is generated in the brewery stage in the beer manufacturing, affording a residue which mainly consists of insoluble proteins, cellulose and lignin. In view of the annual generation of large quantities of this product, for each 100 L of beer production 40 kg of wort bagasse are produced, we have decided to explore this waste carbon source to synthesize C-dots. The oxidation degree of C-dots surface is known to be influenced by the synthetic route.[10] The oxidation process provides sp^3 domain formation on the C-dots surface, resulting in surface decoration with different functional groups, such as carboxyl, carbonyl, hydroxyl and epoxy groups.[11] The presence of these oxygenated functional groups plays important roles on the hydrophilic properties of the C-dot derivatives and also permits the design of more specific bioprobes through simple chemical modifications.[7] The zeta potential values, acquired at pH 5 in aqueous medium, are in the range of −13.3 and −8.89 mV for **1** and **2**, respectively, which are comparable to previous reported values.[12,13] The decrease of zeta potential observed for **2** supports the hypothesis that the surface of **1** is more oxidized and the presence of carboxylate (COO$^-$) groups is in accordance with the idea of a higher oxidation level for **1**.[14]

High-resolution transmission electron microscopy images acquired for **1** and **2** (Figure 1) show well-dispersed particles with spheroidal morphologies. **1** and **2** present narrow size distributions ranging from 2.5-5.9 nm and 2.5-5.3 nm, with average sizes of 4.08 and 3.72 nm, respectively. The inserts in Figures 1a and 1b exhibit representative images of individual particles, indicating the high crystallinity with lattice parameters of 3.13 and 3.15 Å, which correspond to the (002) diffraction plane of graphite.[15] These results show that both synthetic routes result in uniform C-dots nanoparticles with similar size distributions.

The FTIR spectra (Figure S1) of C-dots **1** and **2** show an intense absorption band centered at 3450 cm^{-1} assigned to O−H bonds stretching vibrations. The bands centered at 1630 cm^{-1} were attributed to asymmetrical vibrations of the C=O groups and these at 1380 cm^{-1} assigned to the C−H bending.

Raman spectroscopy provides a powerful diagnostic tool to examine crystallinity.[16] The Raman scattering
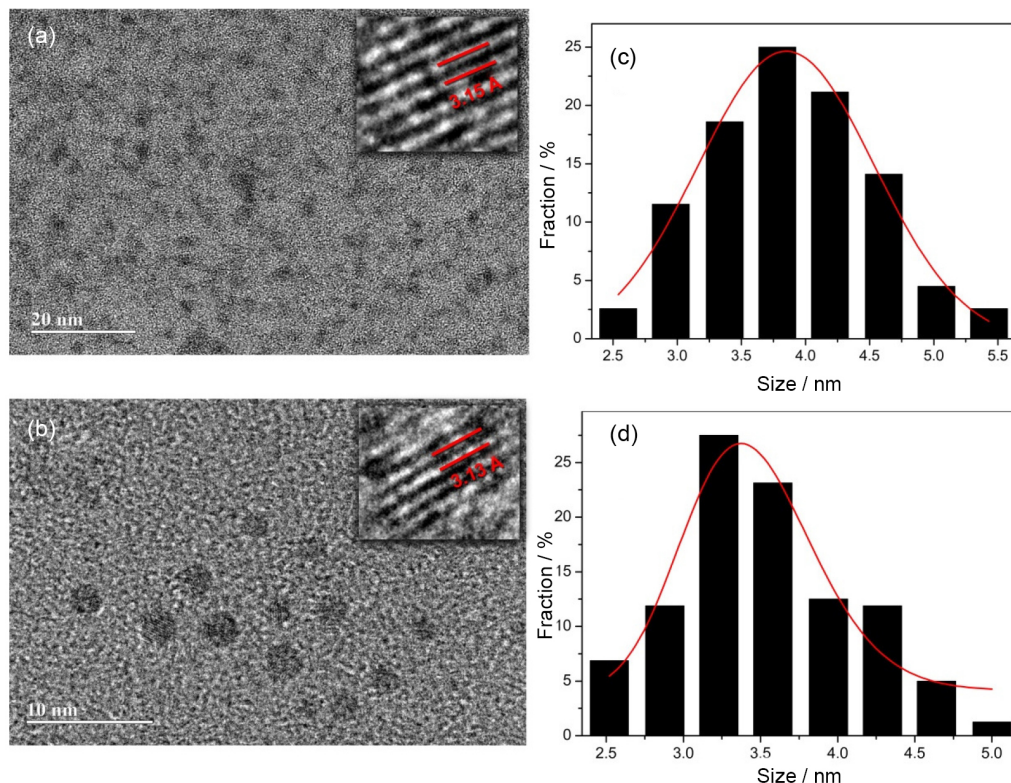
Figure 1. High-resolution transmission electron microscopy (HRTEM) images of C-dots (a) **1** and (b) **2**; and size distribution histograms for (c) **1** and (d) **2**. The inserts in (a) and (b) emphasize the lattice fringes of representative particles.

from C-dots **1** at room temperature (r.t.) is available in the Supporting Information (Figure S2). C-dots **2** exhibited an identical profile. The peaks around 724 and 1068 cm^{-1} correspond to the A_{1g} and E_g modes of the crystalline sodium nitrate, respectively.[17] The other two peaks (1380 and 1577 cm^{-1}) are generally observed in graphite-based materials. The D band (1380 cm^{-1}) exhibits disorder characteristic related to the presence of sp^3 defects, while the peak around 1577 cm^{-1} is attributed to the well-graphitized carbon, which is associated to in-plane vibration of sp^2 carbon atoms in the 2D hexagonal lattice. Thus, the relative intensity ratio of the D-band and G-band (I_D/I_G) provides the degree of disorder, which makes it possible to compare the structural order between crystalline and amorphous graphitic systems.[18,19] The I_D/I_G for the C-dots synthesized in this work was around 0.95, demonstrating that they present a similar graphitic-like structure. Results from Raman experiments proved to be in agreement with those reported for C-dots synthesized from unconventional carbon sources.[5,20,21]

The remarkable optical properties of the C-dots **1** and **2** were confirmed with ultraviolet-visible spectroscopy (UV-Vis) and photoluminescence spectra. The UV-Vis absorption spectra, exhibited in Figure 2, display an intense band at 228 nm, which may be correlated to n-π* transitions. Additionally, low intensity absorption shoulders

were observed at about 305 nm, assigned to π-π* functional group at the surface. The difference in the oxidation degree of C-dots does not alter their absorption profile, thus the energy associated with exciton formation in **1** and **2** are quite similar. The optical band gap, obtained from Tauc and Abeles[22] method, was the same for both materials (5.2 eV). The origin of the optical properties of C-dots is still hotly debated and is yet not well understood. Therefore, mechanisms involving quantum confinement, surface traps, formation of aromatic structures and recombination of excitons have been proposed.[3] The emission spectra of **1** and **2** measured at r.t. are also shown in Figure 2 and display broad bands centered at 460 and 440 nm, respectively.

In Figure 3 is depicted both the emission spectra and the emission intensities as functions of the temperature and pH. C-dots **1** and **2** showed an excitation dependence profile with slightly different spectral behavior. C-dots type **1** exhibited a blue shift of 20 nm (460 to 440 nm) when gradually excited from 300 to 340 nm, whereas between 350-450 nm the emission bands were progressively red shifted by 66 nm (440 to 506 nm). On the other hand, the excitation-dependence of **2** just starts upon excitation at 350 nm, when the emission bands were shifted about 70 nm toward the red spectral range. These results are consistent with the presence of defects at the C-dots surfaces as the net result of distinct oxidation degrees.[10,23]
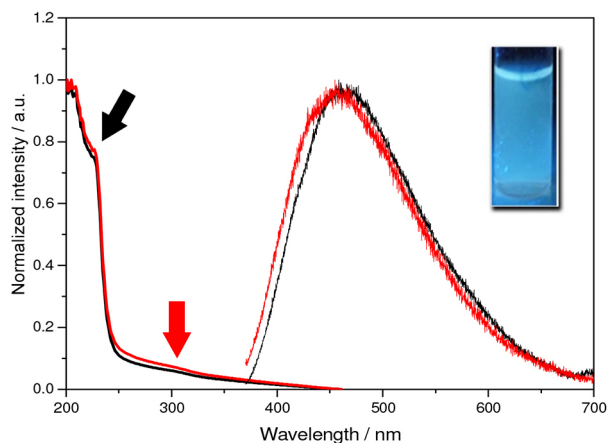
Figure 2. Ultraviolet-visible spectroscopy (UV-Vis) absorption and emission spectra of the C-dots. The solid colored and black lines represent **1** and **2**, respectively. The emission spectra were acquired at r.t. under excitation at 300 nm. Black and colored arrows indicate the n-π^* and π-π^* transitions, respectively. The insert shows **1** under UV light-irradiation (366 nm).

C-dots **1** and **2** show distinct spectral behavior with gradual increasing pH (Figures 2b and 2e). For C-dots type **2**, the pH of aqueous media does not dramatically affects their emission, that is, a fact explained by the low pH-dependence of the functional groups at the C-dots surfaces. On the other hand, the photoluminescence intensity of **1** decreases when the pH values increase and may be justified by the presence of large quantities of carboxylic acid groups on the nanoparticle surface. Under acidic conditions, these functional groups are protonated; and with gradual pH increasing, the Fermi levels can be shifted due to the deprotonation process.[24,25] The temperature effect on the emission intensities of the C-dots are shown in Figures 3c and 3f. The emission intensities of **1** and **2** are progressively diminished as a consequence of multiphoton coupling at higher temperatures, which favors non-radioactive decay.
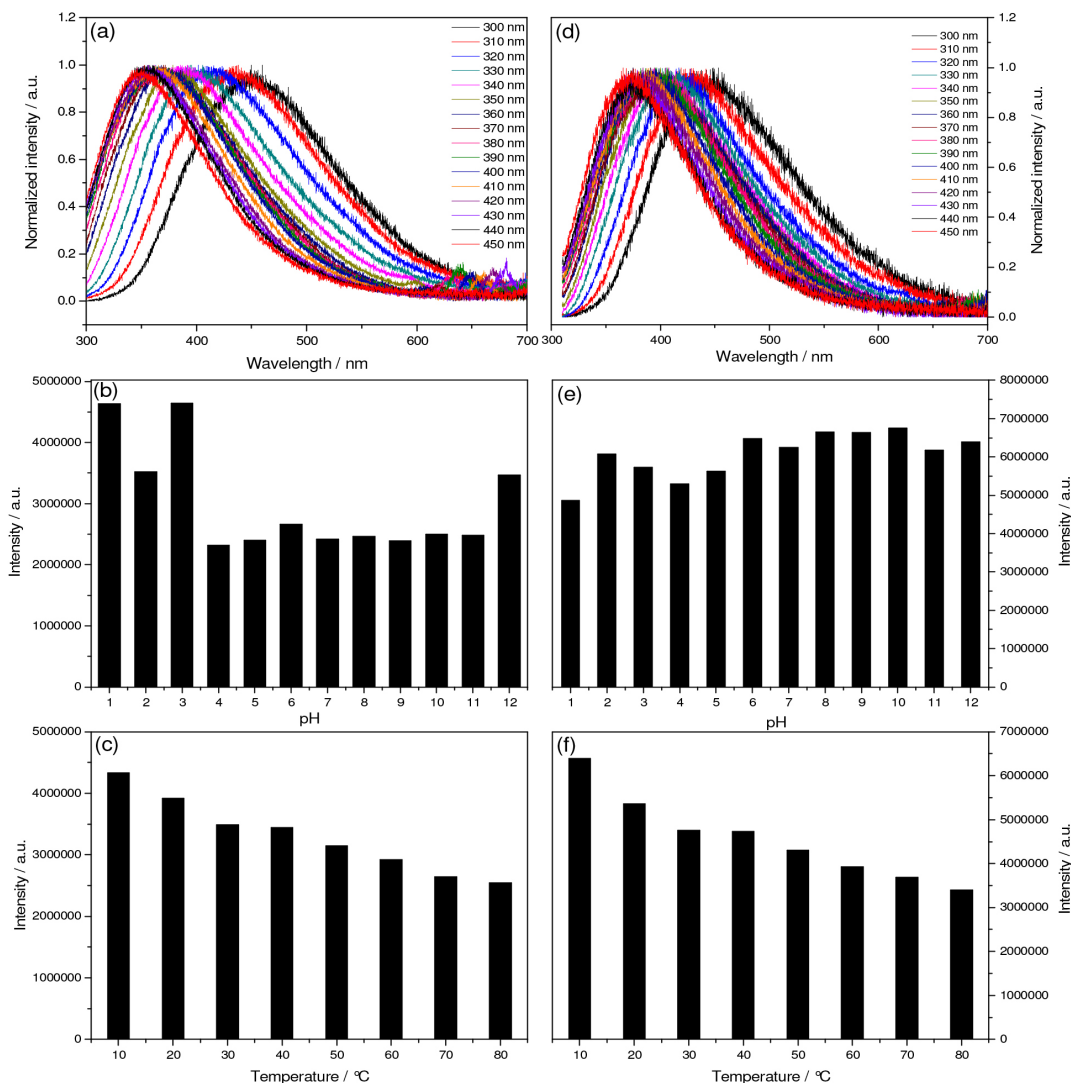

Figure 3. Emission spectra of (a) **1** and (d) **2** acquired at r.t. upon progressive excitation wavelength (from 300 nm to 450 nm); emission intensities as function of pH of (b) **1** and (e) **2** acquired upon excitation at 300 nm; and intensities as a function of the temperature of the analyses for (c) **1** and (f) **2**.
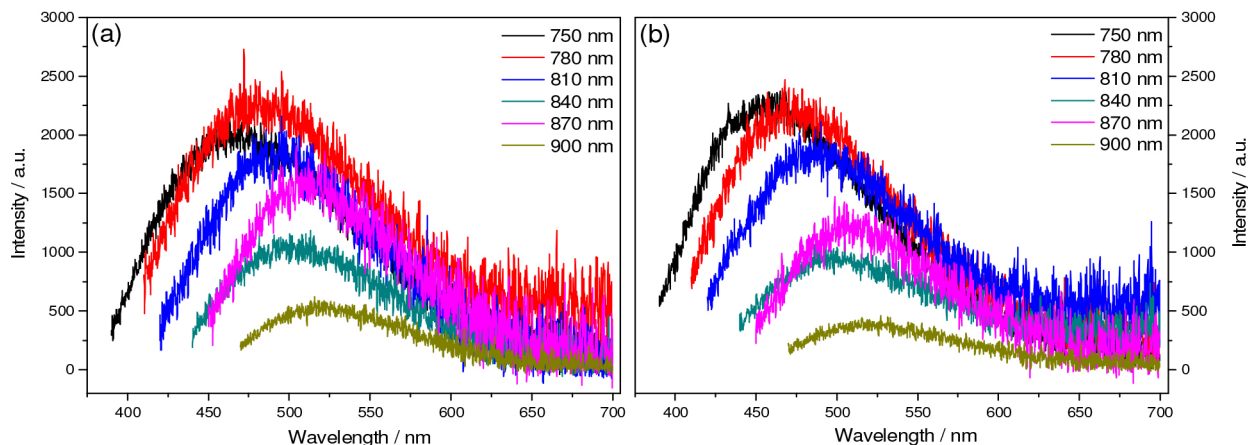
Figure 4. Room temperature up-conversion photoluminescence for (a) **1** and (b) **2** in aqueous media, under pH 6 upon progressive excitation from 750 to 900 nm.

C-dots **1** and **2** also exhibited an interesting up-conversion (UC) photoluminescent emission when excited in the near-infrared (NIR) region, similar to those reported for C-dots from several carbon sources.[26-29] The excitation spectra of **1** and **2** in the NIR region have been acquired monitoring their emission at 460 nm (Figure S3) and displayed two bands centered at 810 and 850 nm, that is, the bands likely to be responsible for the excitation of the materials. Figure 4 displays the UC emission spectra of **1** and **2** acquired at r.t. upon excitation at the NIR region.

The UC emission spectra of **1** and **2** show broad bands centered at 470 and 460 nm when excited at 750 nm. The UC properties may be justified by the combination of two or more low energy photons to produce the emission of a high energy photon. The UC emission spectra still show an excitation dependence behavior, similarly to those previously reported.[25] These results show the potential of these nanomaterials for the development and application of new photocatalyst composites, solar cells, and for applications in cell-imaging with two-photon fluorescence microscopy.

Finally, the more oxidized C-dots **1** were submitted to cell-imaging experiments. **1** has been selected for cell-imaging experiments instead of **2** for a better comparison with previously reported bioimaging experiments reported elsewhere.[4] Figure 5 exhibits the confocal images using breast cancer cells (MCF-7).

A cell cytoplasm staining pattern typical of a non-selective bioprobe was observed for both samples (adhered and live cells). It was also observed a very interesting feature when the cell nuclei were analyzed. C-dots **1** proved to be capable of staining nucleoli selectively, as is shown for the live cell samples. Although the nucleoli staining pattern was very clear with a large bright green emission (Figures 5a and 5d), live and adhered samples also showed a slight staining pattern associated with the cytoplasm region near the nuclei. These characteristics have already
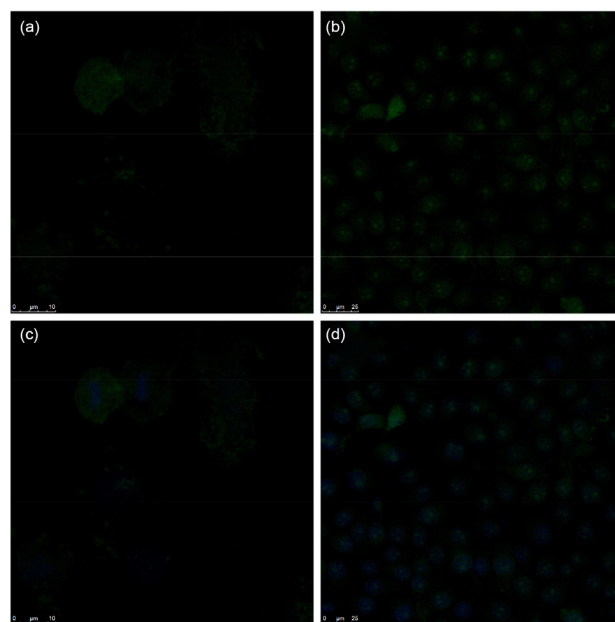

Figure 5. Bioimaging experiments using C-dots type **1** with MCF-7 breast cancer cells. (a) and (b) show the staining patterns (green) for fixed and live cells, respectively; (c) and (d) exhibit overlay between C-dot type **1** and the DNA staining with 4',6-diamidino-2-phenylindole (DAPI). The fluorescent signal is strongly associated with the nucleoli region in live cell samples. C-dots and DAPI are responsible for the green (lighter in printed version) and blue (darker in printed version) emission, respectively. Reference bars: 10 μm to (a) and (c), and 25 μm to (b) and (d).

been described to similar materials reported by Kang and co-workers.[30]

Conclusions

In summary, residues from the brewing industry were successfully used as a carbon source to obtain luminescent C-dots through two facile synthetic procedures. C-dots presented excellent aqueous solubility and similar optical properties. The pH- and temperature-dependence observed for **1** and **2** may be justified by their distinct oxidation

degrees. The C-dots type **1** were tested as a new bioprobe for bioimaging using MCF-7 cancer cells and proved to be more accumulated in the nucleoli region in live cell-imaging experiments. Nucleoli are very activity regions inside the nuclei, which contain several enzyme complexes and play key roles in cellular homeostasis. There are very few molecules commercially available capable of staining nucleoli selectively. The UC photoluminescence exhibited by C-dots and their staining pattern enables their future applications in cell-imagining experiments and provide a new tool to nucleoli studies linked with health and disease conditions through fluorescence microscopy. Bioimaging experiments comparing **1** and **2** are under way and will be disclosed elsewhere.

Supplementary Information

Synthetic procedures and additional experimental details are available free of charge at http://jbcs.sbq.org.br.

Acknowledgements

References

1. Jun, S. S.; Xia, B.; Bok, L. S.; *Drug Discovery Today* **2007**, *12*, 657.

2. Chan, W. C. W.; Maxwell, D. J.; Gao, X.; Bailey, R. E.; Han, M.; Nie, S.; *Curr. Opin. Biotechnol.* **2002**, *13*, 40.

3. Hong, G.; Diao, S.; Antaris, A. L.; Dai, H.; *Chem. Rev.* **2015**, DOI: 10.1021/acs.chemrev.5b00008.

4. Luo, P. G.; Yang, F.; Yang, S. T.; Sonkar, S. K.; Yang, L.; Broglie, J. J.; Liu, Y.; Sun, Y. P.; *RSC Adv.* **2014**, *4*, 10791.

5. Zhou, J.; Sheng, Z.; Han, H.; Zou, M.; Li, C.; *Mater. Lett.* **2012**, *66*, 222.

6. Liu, S.-S.; Wang, C.-F.; Li, C.-X.; Wang, J.; Mao, L.-H.; Chen, S.; *J. Mater. Chem. C* **2014**, *2*, 6477.

7. D'Angelis, E. S. B.; Corrêa, J. R.; Medeiros, G. A.; Barreto, G.; Magalhães, K. G.; de Oliveira, A. L.; Spencer, J.; Rodrigues, M. O.; Neto, B. A. D.; *Chem. - Eur. J.* **2015**, *21*, 5055.

8. Mello, L. R. P. F.; Mali, S.; *Ind. Crops Prod.* **2014**, *55*, 187.

9. Mardegan, S. F.; Andrade, T. M. M.; Sousa Neto, E. R.; Vasconcelos, E. B. C.; Martins, L. F. B.; Mendonça, T. G.; Martinelli, L. A.; *J. Food Compos. Anal.* **2013**, *29*, 52.

10. Bao, L.; Zhang, Z.-L.; Tian, Z.-Q.; Zhang, L.; Liu, C.; Lin, Y.; Qi, B.; Pang, D.-W.; *Adv. Mater.* **2011**, *23*, 5801.

11. Zhu, S.; Zhang, J.; Liu, X.; Li, B.; Wang, X.; Tang, S.; Meng, Q.; Li, Y.; Shi, C.; Hu, R.; *RSC Adv.* **2012**, *2*, 2717.

12. Wu, L.; Luderer, M.; Yang, X.; Swain, C.; Zhang, H.; Nelson, K.; Stacy, A. J.; Shen, B.; Lanza, G. M.; Pan, D.; *Theranostics* **2013**, *3*, 677.

13. Lotya, M.; Hernandez, Y.; King, P. J.; Smith, R. J.; Nicolosi, V.; Karlsson, L. S.; Blighe, F. M.; De, S.; Wang, Z.; McGovern, I.; *J. Am. Chem. Soc.* **2009**, *131*, 3611.

14. Krishnamoorthy, K.; Veerapandian, M.; Yun, K.; Kim, S.-J.; *Carbon* **2013**, *53*, 38.

15. Wang, G.; Yang, J.; Park, J.; Gou, X.; Wang, B.; Liu, H.; Yao, J.; *J. Phys. Chem. C* **2008**, *112*, 8192.

16. Yadav, R. M.; Dobal, P. S.; Shripathi, T.; Katiyar, R. S.; Srivastava, O. N.; *Nanoscale* **2009**, *4*, 197.

17. Rousseau, D. L.; Miller, R. E.; Leroi, G. E.; *J. Chem. Phys.* **1968**, *48*, 3409.

18. Wu, M.; Wang, Y.; Wu, W.; Hu, C.; Wang, X.; Zheng, J.; Li, Z.; Jiang, B.; Qiu, J.; *Carbon* **2014**, *78*, 480.

19. Bagga, K.; McCann, R.; Wang, M.; Stalcup, A.; Vazquez, M.; Brabazon, D.; *J. Colloid Interface Sci.* **2015**, *447*, 263.

20. Hsu, P.-C.; Chang, H.-T.; *Chem. Commun. (Cambridge, U. K.)* **2012**, *48*, 3984.

21. Hsu, P.; Shih, Z.; Lee, C.; Chang, H.; *Green Chem.* **2012**, *14*, 917.

22. Tauc, J. In *Optical Properties of Solids*; Abeles, F., ed.; American Elsevier: New York, 1972, ch. 5.

23. Zhu, S.; Zhang, J.; Tang, S.; Qiao, C.; Wang, L.; Wang, H.; Liu, X.; Li, B.; Li, Y.; Yu, W.; *Adv. Funct. Mater.* **2012**, *22*, 4732.

24. Zhao, W.; Song, C.; Pehrsson, P. E.; *J. Am. Chem. Soc.* **2002**, *124*, 12418.

25. Jia, X.; Li, J.; Wang, E.; *Nanoscale* **2012**, *4*, 5572.

26. Cao, L.; Wang, X.; Meziani, M.; Lu, F.; Wang, H.; Luo, P.; Lin, Y.; Harruff, B.; Veca, L.; Murray, D.; *J. Am. Chem. Soc.* **2007**, *129*, 11318.

27. Li, H.; He, X.; Kang, Z.; Huang, H.; Liu, Y.; Liu, J.; Lian, S.; Tsang, C. H. A.; Yang, X.; Lee, S. T.; *Angew. Chem., Int. Ed.* **2010**, *49*, 4430.

28. Zhuo, S.; Shao, M.; Lee, S.; *ACS Nano* **2012**, *6*, 1059.

29. Yin, B.; Deng, J.; Peng, X.; Long, Q.; Zhao, J.; Lu, Q.; Chen, Q.; Li, H.; Tang, H.; Zhang, Y.; *Analyst (Cambridge, U. K.)* **2013**, *138*, 6551.

30. Kong, W.; Liu, R.; Li, H.; Liu, J.; Huang, H.; Liu, Y.; Kang, Z.; *J. Mater. Chem. B* **2014**, *2*, 5077.